Spin-coated synthesis of polyvinylidene fluoride-barium titanate nanocomposite piezoelectric flexible thin films.

KANIAPAN, S., PRATHURU, A. and FAISAL, N.

2024

Spin-coated synthesis of polyvinylidene fluoride-barium titanate nanocomposite piezoelectric flexible thin films

Sivabalan Kaniapan[*a], Anil Prathuru[a], Nadimul Faisal[a]

[a]School of Engineering, Robert Gordon University, Garthdee Road, Aberdeen, AB10 7GJ, UK

ABSTRACT

Energy derived from mechanical deformation is one of the cleaner energy options known as piezoelectric. Polyvinylidene fluoride (PVDF) has been identified to hold the characteristics of piezoelectric and dielectric properties due to good energy storage capacity and electrical breakdown strength. However, lower piezoelectricity limits its applicability, and therefore, advancement is needed, potentially through doping or filler like barium titanate (BaTiO$_3$ or BTO). Several fabrication approaches have been proposed, yet spin coating is desirable vis. for its reliability, ease of replicable, cost-effectiveness, and uniform coating. In this study, thin films were fabricated using spin coating with 5 wt.% and 12 wt.% BTO/PVDF compositions at 1000 rpm and 4000 rpm. The morphological characteristics of the materials were studied using Fourier transform infrared (FTIR) and scanning electron microscope (SEM) analysis techniques. The results showed that the 5wt.% BTO/PVDF film at 4000 rpm and annealed at 120 °C for 6 hours exhibited a maximum relative beta (β) fraction of around 94%. SEM images revealed the uniform distribution of BTO particles with less agglomeration in the PVDF matrix, indicating that adding BTO promotes nucleation sites for forming a more ordered crystalline structure. Despite that, further validation of crystallinity percentage is required to assess the enhancement made by the BTO fillers in a polymer matrix entirely. Overall, the experiment demonstrated that spin coating can effectively enhance the β-phase of PVDF (β-phase is desirable due to relatively high dielectric constant and piezoelectricity) with the addition of ceramic fillers such as BTO.

Keywords: relative beta fraction, morphological characteristics, crystal orientation, crystallinity, polyvinylidene fluoride, nucleation, piezoelectric

1. INTRODUCTION

The supremacy and the need for energy have substantially increased over the last few centuries, creating huge impacts such as energy crises and global warming, necessitating the exploration of sustainable and cleaner energy production. Among these options, energy derived from mechanical deformation is one of the cleaner energy options known as piezoelectric. In general, a piezoelectric material is a self-powered innovative component that converts mechanical energy or force into an electric charge or vice versa. This dual characteristic of piezoelectric material has widespread application in various industries as sensors or actuators. Extensive research has been conducted on the implementation of piezoelectric materials in harvesting power and thermal energy [1], [2], structural health monitoring [3], biomedical devices such as bone regeneration [4], pacemaker [5], glucose level monitoring [6] and tuberculosis detection [7].

Polyvinylidene (PVDF) has been identified as one of the electroactive semicrystalline materials that holds the characteristics of piezoelectric properties. It is a self-powered, anisotropic, and ferroelectric smart material with compelling properties such as lightweight, smoothness, malleability, non-toxic, mechanical, and thermal stability, making it an ideal candidate for multidisciplinary field applications. However, lower piezoelectricity limits its applications, and enhancement is needed with doping or filler like barium titanate (BTO) [8]. The incorporation of fillers improves the sensitivity and performance to optimise piezoelectric characteristics and functionality. Yet, the enhancement of piezoelectric properties depends on the selection of the fabrication method.

In addition, several fabrication methods have been demonstrated by many researchers in the past, such as hot embossing, electrospinning, and spin coating. These techniques were apparent to several constraints, such as agglomeration due to heterogeneous dispersion of inorganic materials, affecting the performance of piezoelectric sensors [9]. Nevertheless, spin coating is desirable vis. its reliability and easily replicable fabrication method favouring integration ease of existing fabrication workflows with process repeatability, cost-effectiveness, and uniform coating. The spin coating can be conducted under different atmospheric temperatures and pressures with lesser equipment complexity. Lastly, the spin coating provides uniform film thickness, making it a preferred choice for piezoelectric fabrication.

In the spin coating technique, the prepared solution is spread thinly onto a substrate with the centrifugal force created by the spin coater instrument when it starts to operate. There are various parameters that need to be considered to form an effective thin coating on the substrate, such as different rotational speed [10], baking and annealing temperature [11], the ageing process, etc., significantly improves the power output and piezoelectricity of the material.

Increasing the spinning speed of the spin coating affects thickness and uniformity, phase content, evaporation rate, morphological characteristics, and film quality. [12] found that films spun at speeds up to 3000 rpm showed an increase in β-phase content, attributed to the stretching effect caused by centrifugal force during spin coating. Nevertheless, films spun at 4000 rpm exhibited a decrement in β-phase content due to the potential permanent destruction of molecular chains.

[13] and his team have compared their experimental analyses with grey theory predictions. They used PVDF as the material with three different weight percentages of 10 %, 15 %, and 20 % in DMF solvent. Additionally, they employed different spin coating speeds of 1000 to 3000 rpm along with varying duration of spin and annealing temperatures of 10 –30 s and 30 - 50 °C, respectively. The microstructure characterisation, conducted through FTIR, XRD, and Atomic Force Microscopy (AFM), revealed that the grey theory prediction elevated the intensity of the β-phase by enabling stretching possibilities of PVDF at higher spin speeds, which resulted in thinner films measuring 2.25 µm and roughness of 3 nm, respectively [13]. In addition, the optimised parameters of 3000 rpm with 10 wt. % of PVDF and 50 °C annealing temperature produce the highest β-phase percentage, resulting in a thinner film with less surface roughness [13].

A recent research article by [14] used spin coating fabrication techniques to characterise P(VDF-HFP)-BTO nanocomposite films, exploring their dielectric properties, temperature dependence, and crystallinity. The study reveals that the flexibility of P(VDF-HFP) increases, whereas crystallinity and elastic modulus decrease with the addition of 15% HFP copolymer. Also, it has been reported that a 15% addition of HFP almost 4 times increment addition of BTO nanoparticles to P(VDF-HFP) polymer matrix increases the dielectric constant and decreases the crystallinity of the composite material [1].

[15] studied the impact of PVDF concentration, spinning speed, spinning duration, and annealing temperature on the computation of relative β-phase percentage, roughness, and thickness of thin films using the L_9 orthogonal Taguchi method. According to the experiment, an optimum concentration of 10 wt. % PVDF, a rotational speed of 3000 rpm, a spinning duration of 30 seconds, and annealing at 70°C resulted in an 86 % relative fraction of β-phase [15]. Furthermore, the microstructure characterisation revealed that higher spinning speeds and higher annealing temperatures favoured thinner films with smoother surfaces than lower spinning speeds and annealing temperatures.

In contrast, [16] claims that using the lowest spinning rate in film preparation intensified the peak intensity. This means a phase intensity reduction can be witnessed at 1000 rpm. However, no significant change was observed for films prepared at 2000 and 400 rpm. The increase in the intensities of the peaks at a low spinning rate of 500 rpm shows an increase in the β-phase (82.6%) in PVDF films. At low spinning rates, more beta-phase forms in PVDF chains due to trans-conformation (reorientation) and low solvent evaporation [16]. Conversely, high spinning rates hinder molecular chain rearrangement.

Although, there are a vast number of approaches with different parameters that have been stipulated by many scholars enhancing piezoelectric properties through the spin coating fabrication method. Yet, more clarity must be clarified with studies that contemplated an opposite result stipulating the same parameter. Additionally, only a few researchers have articulated using fillers such as BTO through the spin coating process. Therefore, this research article sheds new light on the explanation for identifying the presence of β- phase through thorough morphological characteristics studies with the addition of fillers (BTO) within the PVDF matrix.

2. METHODOLOGY

The methodology has been subdivided into a few categories, as shown in Figure 1. The first section describes the material selection, where three fundamental materials were used in the experiment: PVDF, BTO, and DMF, which were procured from Sigma Aldrich without any further purification. The molecular weight of M_w= 534 000, 233.19, and 58.08 of PVDF, BTO, and DMF is based on the technical datasheets supplied by the chemical manufacturer, respectively. Next, the solution preparation method is followed by spin coating and post-thermal treatment. Further, all the samples were analysed through Fourier Transform Infrared (FTIR) and scanning electron microscope (SEM) to determine the percentage of β- phase and morphological characteristics, respectively.
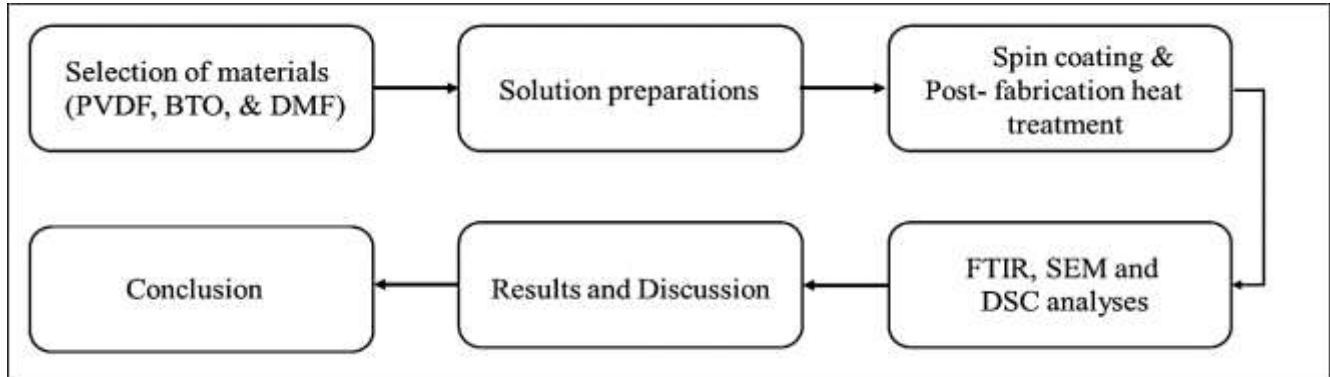
Figure 1. The block diagram of the experimental process flows

2.1 Solution preparation

The initial process of the experiment was to prepare a polymer solution of a 1:9 ratio or, in other words, a weighing measurement of 10 wt. % PVDF/DMF concentration. A digital weighing scale of Mettler Toledo™ Standard ME Analytical Lab Balance from Fisher Scientific was chosen for precise measurement. Beakers used for the experiment were cleaned with deionised water and an acetone solution to prevent dust and fine contaminants before weighing PVDF. The beaker containing the PVDF/DMF solution was then placed in a water bath to avoid direct heating from the magnetic stirrer. The prepared solution placed in a water bath was heated at room temperature until the sample reached 80 °C to ensure thermodynamic equilibrium. This is to ensure the low viscosity of the solution and create enough thermal energy associated with the CF_2 group rotation through a large-scale conformational change of α to β is formed [20]. Also, very small crystallites exist at low temperatures due to partial dissolution or refolding of the polymer chains, which serve as nuclei when the solution is recrystallised [21]. Next, the solution was agitated using a magnetic stirrer at the desired rotational speed to prevent agglomeration of PVDF particles in the DMF solvent for approximately 45 min or until all the PVDF particles were evenly distributed without any lumps. The miscible polymer solution is ready for spin-coating and subsequent thermal treatment. Next, a composite solution is prepared with the addition of BTO (5wt. % and 12 wt %) into the polymer solution and stirred for another 45 minutes. This is followed by ultrasonication at room temperature for 20 minutes to make sure that the BTO is well incorporated with the PVDF solution. It has been clearly stated that there are two magnetic stirring processes before and after the addition of BTO, as shown in Table 1.

Table 1. Solution preparation with specific weight ratios of PVDF, BTO, and DMF

Sample	Solution preparation, (g)			Magnetic				Ultrasonication, (m)	
	PVDF	DMF	BTO	Before		After			
				D, (m)	T, °C	D, (m)	T, °C	T, °C	D, (m)
(1)	10	90	0	45	80	45	80	RT	20
(2)	10	90	0.5263	45	80	45	80	RT	20
(3)	10	90	1.3636	45	80	45	80	RT	20

Note: duration (D), time (T)

2.2 Spin coating and post-fabrication heat treatment

In this study, thin films were fabricated using spin-coating technique. The model used for this analysis is the spin coater series (SCS 6800) by Kisco Specialty Coating Systems, USA. The process of spin coating starts with nitrogen gas (N_2) purging, approximately at a pressure of around two bar. Whilst the N_2 purging, the spin coater machine was set according to experimental designs or setups. The prepared polymer solution of 10 wt. % PVDF/DMF and composite solutions of 5 wt. % BTO/PVDF and 12 wt. % BTO/PVDF were spin-coated at spin speeds of 1000 rpm and 4000 rpm. All the samples were prepared by choosing a constant ramp and dwell duration parameters of 10 seconds and 30 seconds.

The coated samples were processed further with post-fabrication heat treatment (annealing). In the current research analysis and with the prior knowledge from the literature reviews, we have chosen a post-heat treatment (annealing) at 80 °C, 100

°C and 120 °C for 6 hours using a BINDER vacuum oven followed by cooling at room temperature for efficient optimisation of crystal structure transformation from α to β conformation [17]–[19]. Additionally, annealing activates the doping elements or the introduction of other impurities in the polymer to tailor for specific properties or functionality of the piezoelectric material for later use [20], [21].

2.3 Microstructure characterisation

The morphological characteristics were studied using Fourier transform infrared (FTIR) and scanning electron microscope (SEM) analysis techniques. The Fourier transform infrared measurement provides information on the material's wavenumbers or conformation of crystalline phases such α, β, and γ. The study was performed via a Thermo Scientific Nicolet iS50 FTIR spectrometer in the range of 400-1500 cm^{-1} with a 2cm^{-1} resolution, which generates transmittance vibrations with different wavenumbers. The degree of α and β conformation, assuming the IR absorption, follows Beer's law. The α-phase had a characteristic infrared absorption at 763 cm^{-1}, and the peak 840 cm^{-1} absorption band is uniquely characteristic of the β-phase.

Following the α, ɤ, and β-phase conformations through the FTIR method, the relative fraction of β-phase F(β) of each sample prepared using spin coating techniques was computed using the Beer−Lambert law estimation as follows [22]:

$$F_\beta = \frac{A_\beta}{1.3A_\alpha + A_\beta} \tag{1}$$

Further, the samples were analysed through differential scanning calorimetry (DSC) to compute the crystallinity percentage. The selected samples were heated from -50 °C to 200 °C, completing the first cycle of heating, followed by subsequent cooling at -50 °C, and lastly, reheating at 200 °C. The samples were heated twice to eliminate thermal history. The obtained DSC results were used to determine the percentage of crystallinity using the following equation:

$$x_c, \% = \frac{\Delta H_m}{(1-\varphi)\Delta H_m^0} \times 100\% \tag{2}$$

Where, x_c is the crystalline percentage, ΔH_m and ΔH_m^0 is the enthalpy of fusion of the sample and enthalpy of fusion of 100% PVDF (103.4 Jg^{-1}), respectively. Whereas, φ represents the percentage of filler in the prepared piezo-composite solution.

3. RESULTS AND DISCUSSION

Based on the experiment, the FTIR results revealed the presence of α, β, ɤ, and ɤ+β crystalline structures in the spin-coated samples. A similar trend of twelve vibrational peaks was observed during FTIR on spin-coated samples of 10 wt. % PVDF/DMF (1), 5 wt. % BTO/PVDF (2) and 12 wt. % BTO/PVDF (3) at 1000 and 4000 rpm. Peaks of 509 cm^{-1} (CF$_2$ stretching) and 840 cm^{-1} (CH$_2$ rocking, CF$_2$ stretching, and skeletal C-C stretching) belong to (ɤ+β or ɤ) crystalline phases. Whereas peaks 736 cm^{-1} and 1235 cm^{-1} are regarded as exclusive α and γ crystalline phases. Additionally, peaks such as 1400 cm^{-1}, 1175 cm^{-1}, 1070 cm$^{-1,}$ and 875 cm^{-1} correspond to all typical phases of (α, β, or γ) depending on the experimental conditions [23]. Other peaks, such as 431 cm^{-1} and 482 cm^{-1}, indicate the presence of exclusive ɤ and α. Also, a peak of 1275 cm^{-1} was present, which correlates with an exclusive β phase. A unique peak of 600 cm^{-1} can be witnessed in all the samples (1) but almost completely vanished in samples (2) and (3) at both spinning speeds of 1000 rpm and 4000 rpm, annealed at 80 to 120 °C (Figure 2b). This particular peak belongs to β-phase (CF$_2$ wagging) [24]. However, this peak could not be taken into consideration as the presence of β phase as this peak appears as α phase due to an intensive peak of 613 cm^{-1} [25]. On the other hand, a peak of 482 cm^{-1} (α), present in all the samples (1), was shifted to 476 cm^{-1} with the addition of BTO. Peak 476 cm^{-1} is an exclusive β-phase. Other significant shifts of peaks were also noticeable with the addition of BTO, such as 431 cm^{-1} (ɤ) to 435 cm^{-1} (β). There are some shifts in specific peaks, such as (509 cm^{-1}, 1175 cm^{-1}, 1235 cm^{-1}, 1275 cm^{-1}, and 1400 cm^{-1}) to (511 cm^{-1}, 1168 cm^{-1}, 1232 cm^{-1}, 1273 cm^{-1}, and 1403 cm^{-1}) with the addition of BTO particles in PVDF solution.

However, the relative beta fraction is computed through two main peaks of 763 cm^{-1} and 840 cm^{-1}, corresponding to α and β phases. Yet, in order to accurately identify the transition from α to β conformation, it is essential to observe the presence of a 1275 cm^{-1} peak, indicating an exclusive β-phase [23]. In regards to phase identification, [23] has substantially divided the peaks into three main groups: 1) exclusive peaks, 2) common peaks, and 3) dual peaks. Exclusive peaks of (445 cm^{-1}, 476 cm^{-1}, and 1275 cm^{-1}) belong to β, (482 cm^{-1}, 431 cm^{-1}, 811 cm^{-1}, and 1234 cm^{-1}) belong to ɤ and (410 cm^{-1}, 489 cm^{-1}, 532 cm^{-1}, 614 cm^{-1}, 763 cm^{-1}, 795 cm^{-1}, 854 cm^{-1}, 975 cm^{-1}, 1149 cm^{-1}, 1209 cm^{-1}, 1383 cm^{-1}, and 1423) belong to α. Whereas 876-885 cm^{-1}, 1067-1075 cm^{-1}, 1171-1182 cm^{-1}, and 1398-1404 cm^{-1} indicate the presence of all three phases of

(α, β, or γ). There were also dual-phase peaks, such as 840 cm^{-1} and 510 cm^{-1}, noted as (β and/ or ɣ) phases [23]. In addition to the past literature review, the current FTIR observation depicts that the presence of an exclusive β phase increases as the annealing temperature increases from 80 °C to 120 °C for both composite and polymer samples. Further, a missing peak of 1275 cm^{-1} indicates the absence of an exclusive β phase on the sample (1) at 1000 rpm compared to 4000 rpm. The exclusive β phase is present later in the sample (1) with an increase in annealing temperature from 80 °C to 120°C. However, with the addition of BTO, even at the lowest spinning speed of 1000 rpm, there is a noticeable 1275cm^{-1} (weak) peak, which becomes stronger with a higher spinning speed of 4000 rpm. Therefore, for sample (1), the exclusive β phase only becomes apparent later with an increase in spinning speed and annealing temperature from 1000 rpm to 4000 rpm and 80 °C to 120 °C, respectively (Figure 2a). Sample (1) at a lower spinning speed (1000rpm) with a lower annealing temperature (80 °C) was considered as the combination of (β+ɣ) representing a peak 840cm^{-1}. On the contrary, for samples (2) and (3), the 1275 cm^{-1} peak was prominent for both high and low annealing temperatures and spinning speeds. On top of that, there is clear evidence of a peak shift of 482 cm^{-1} (α) to 473 cm^{-1} (β) and 431 cm^{-1} (ɣ) to 435 cm^{-1} (β), which ascribe the transition of α and ɣ phases to β phase with the addition of BTO.

The relative beta fraction of all the spin-coated samples was increased as the spinning speed increased, as shown in Figure 2c. The lowest relative beta fraction of approximately 75 % was found with sample (3) annealed at 100 °C. However, this decrement in the computed β percentage is just momentarily as further increase in temperature increases the relative beta fraction. This phenomenon is due to the incomplete evaporation of DMF solvent, which hinders the crystallisation of PVDF [26]. Further, an increase in BTO causes agglomeration of BTO particles within the PVDF matrix, which reduces the α to β transition [27]. A higher relative beta fraction (94%) was obtained from a 4000 rpm spin-coated sample (2) annealed at 120 °C for 6 hours.

On the other hand, the DSC analysis revealed a slight variation in the melting temperature of sample (2) under different annealing temperatures of 80 °C to 120 °C. A sample annealed at 80 ℃ showed a melting peak at 157.47 ℃ which increased to 157.62 °C for a sample annealed at 100 °C and dropped to 156.98 ℃ for a sample annealed at 120 ℃ as shown in Figure 3a. This is mainly due to the increase in crystalline sizes (growth in lamellar and nucleation promotions) as the annealing temperature increases. However, a further increase in annealing temperature to 120 ℃ causes melting in the crystallisation zone, which eventually decreases the crystallinity of the sample [28], which was proven by the drop in the percentage of crystallinity from 25.51 % to 23.66 % for samples annealed at 80 °C and 120 °C, respectively. Additionally, further exothermic cooling processes of DSC deduce that the crystallisation peaks appear at 132.46 ℃, 132.13 ℃, and 131.83 ℃ for samples annealed at 80 ℃ to 120 ℃ (Figure 3b).

Lastly, the SEM analysis revealed a direct correlation between spinning speed and porosity, with an increase in spinning speed leading to higher porosity in the samples. Additionally, the SEM images displayed a uniform distribution of BTO particles across the sample, although some areas exhibited agglomeration of these particles. Notably, the identification of these agglomerated spots as the addition of BTO particles increases from 5 % in the sample (2) to 12 % in the sample (3) (Figures 4c and 4d). The SEM images of PVDF composite films spun at varying speeds illustrated microscopic pores and oriented fibrils between spherulites. This was particularly evident at higher spin speeds due to lower viscosities, allowing for more significant centrifugal forces on the molecular chains. The morphologies depicted rough surfaces and micro-pore structures, indicating interactions between the solvent and polymer matrix, which was also evident in other research articles [29]. Porosity increased with escalating spinning rates from 1000 rpm to 4000 rpm (Figures 4a and 4b), leading to difficulties in further processing, such as poling and electrode plating.

In this study, the FTIR analysis of the sample with higher annealing temperatures shows higher fractions of relative beta percentage due to the use of a vacuum oven for the annealing process. Whereby annealing using a vacuum oven induces rapid crystallisation and forms a skin on the top layer of the sample, which traps the solvent and prevents solvent evaporation. In relation, this process causes the formation of β content with a drawback of possible electroactive degradation of the sample. Nonetheless, the process of finding the percentage of the sample's crystallinity through DSC was computed using the enthalpy of fusion in regard to the exothermic process. This percentage of crystallinity represents the small sample used during the DSC analyses, which were roughly about 5 to 10mg. Additionally, FTIR analysis depicts crystalline peaks, and the computation of crystal percentage is only a fraction basis of β to α phases. This percentage is a small area representation of the sample during the FTIR analysis and not the whole fabricated piezoelectric film. Therefore, the overall methodology can be improved further in future work through the X-ray diffraction method (XRD) in computing the final crystallinity percentage of the sample, and the distribution of filler particles can be controlled by controlling the grain size.
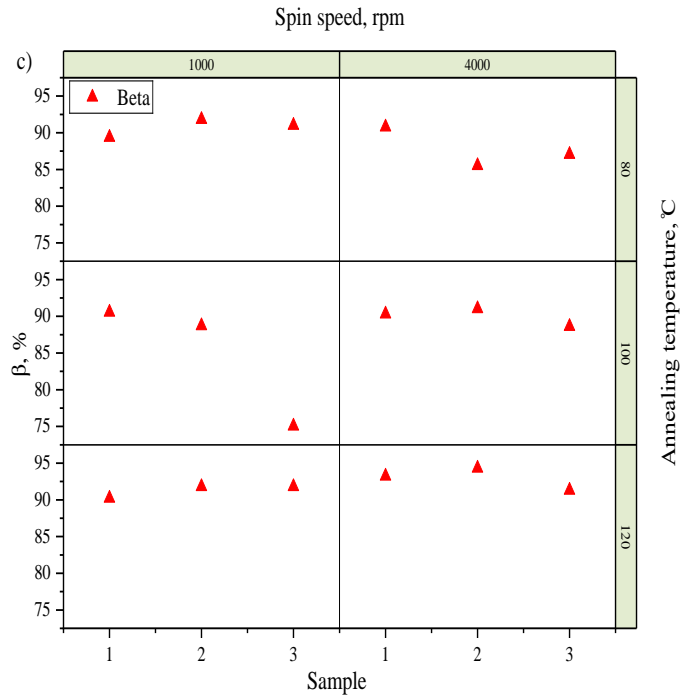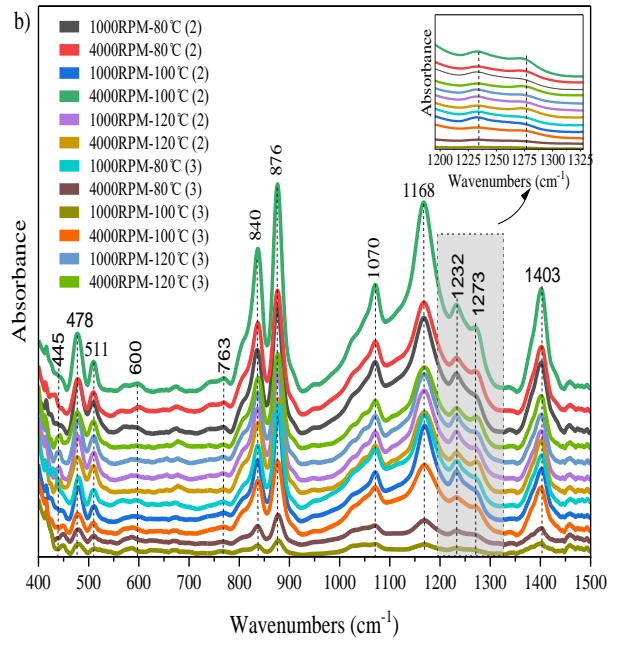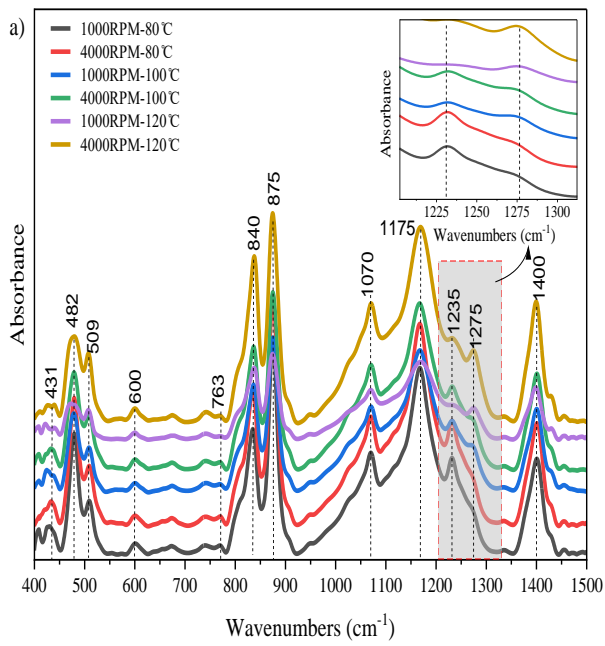
Figure 2. Spin coated at 1000 rpm and 4000 rpm of a) 10 wt. % neat PVDF, b) 5 wt. % BTO/PVDF and 12 wt. % BTO/PVDF; c) relative β %
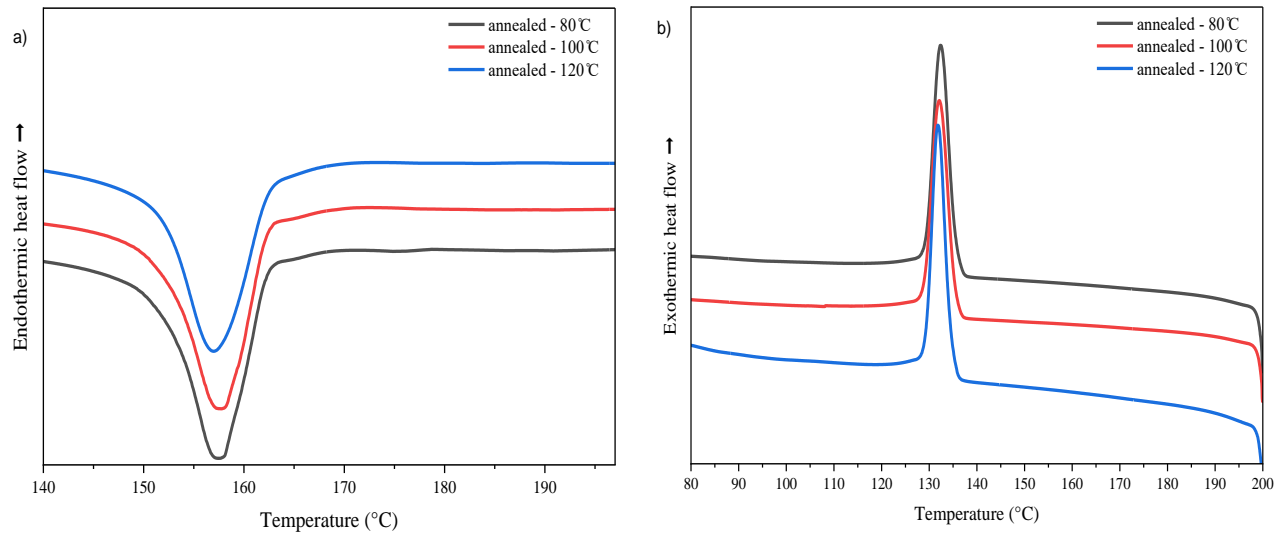
Figure 3. DSC analysis of samples annealed at 80 ℃ to 120 ℃ of a) Melting process and b) cooling process
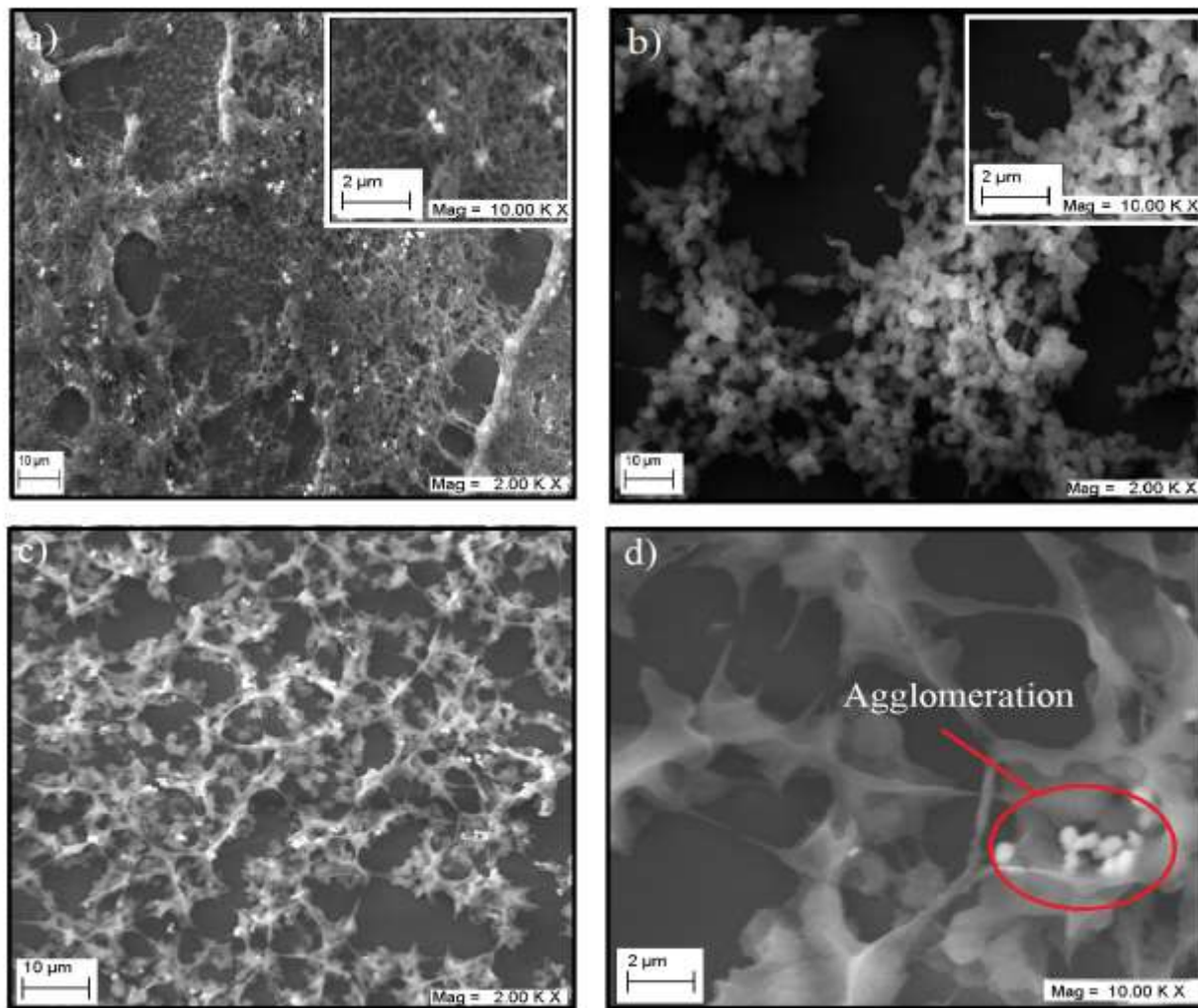

Figure 4. SEM analyses of a) sample (2) with 1000 rpm, b) sample (2) with 4000 rpm, c) sample (3) with 4000 rpm, and d) sample (3) with 4000 rpm at 10X magnification

4. CONCLUSION

There is still room for improvement in terms of different parameter selections, doping concentration, solvent selection, and concentration, as well as post-fabrication poling treatment. Thus, using spin coating is an ideal strategy, and the results showed that the 5 wt.% BTO/PVDF film at 4000 rpm and annealed at 100 °C for 6 hours exhibited a maximum relative beta fraction of 94%. SEM images revealed the uniform distribution of BTO particles with less agglomeration in the PVDF matrix, which indicates that the addition of BTO promotes nucleation sites for the formation of a more ordered crystalline structure. However, validation of crystallinity percentage is required to fully assess the enhancement made by the BTO fillers in the polymer matrix. Therefore, the experiment demonstrated that spin coating speed and annealing temperature variations can enhance the beta phase with the addition of ceramic fillers such as BTO.

ACKNOWLEDGEMENTS

REFERENCES

[1]   J. Boughaleb *et al.*, "Coupling of PZT thin films with bimetallic strip heat engines for thermal energy harvesting," *Sensors (Switzerland)*, vol. 18, no. 6, Jun. 2018, doi: 10.3390/S18061859.

[2]   Y. Meng, G. Chen, and M. Huang, "Piezoelectric materials: Properties, advancements, and design strategies for high-temperature applications," *Nanomaterials*, vol. 12, no. 7, Apr. 2022, doi: 10.3390/NANO12071171.

[3]   P. Jiao, K. J. I. Egbe, Y. Xie, A. M. Nazar, and A. H. Alavi, "Piezoelectric sensing techniques in structural health monitoring: A state-of-the-art review," *Sensors (Basel).*, vol. 20, no. 13, pp. 1–21, Jul. 2020, doi: 10.3390/S20133730.

[4]   A. Carter, K. Popowski, K. Cheng, A. Greenbaum, F. S. Ligler, and A. Moatti, "Enhancement of bone regeneration through the converse piezoelectric effect, a novel approach for applying mechanical stimulation," *Bioelectricity*, vol. 3, no. 4, pp. 255–271, Dec. 2021,
doi: 10.1089/BIOE.2021.0019/ASSET/IMAGES/LARGE/BIOE.2021.0019_FIGURE3.JPEG.

[5]   Z. Yi *et al.*, "A battery- and leadless heart-worn pacemaker s trategy," *Adv. Funct. Mater.*, vol. 30, no. 25, pp. 1–9, 2020, doi: 10.1002/adfm.202000477.

[6]   X. Xue, Z. Qu, Y. Fu, B. Yu, L. Xing, and Y. Zhang, "Self-powered electronic-skin for detecting glucose level in body fluid basing on piezo-enzymatic-reaction coupling process," *Nano Energy*, vol. 26, pp. 148–156, 2016, doi: 10.1016/j.nanoen.2016.05.021.

[7]   J. Zhang and F. He, "Mycobacterium tuberculosis piezoelectric sensor based on AuNPs-mediated enzyme assisted signal amplification," *Talanta*, vol. 236, no. July 2021, 2022, doi: 10.1016/j.talanta.2021.122902.

[8]   H. Kim, F. Torres, D. Villagran, C. Stewart, Y. Lin, and T. L. B. Tseng, "3D Printing of BaTiO3/PVDF Composites with Electric In Situ Poling for Pressure Sensor Applications," *Macromol. Mater. Eng.*, vol. 302, no. 11, Nov. 2017, doi: 10.1002/MAME.201700229.

[9]   S. Duan, J. Wu, J. Xia, and W. Lei, "Innovation Strategy Selection Facilitates High-Performance Flexible Piezoelectric Sensors," *Sensors (Basel).*, vol. 20, no. 10, May 2020, doi: 10.3390/S20102820.

[10]   D. G. Jeong, H. H. Singh, M. S. Kim, and J. H. Jung, "Effect of Centrifugal Force on Power Output of a Spin-Coated Poly(Vinylidene Fluoride-Trifluoroethylene)-Based Piezoelectric Nanogenerator," *Energies*, vol. 16, no. 4, p. 1892, Feb. 2023, doi: 10.3390/EN16041892/S1.

[11]   Marut Khieokae; Kanut Jinpak; Suphattra Kritwattanakorn; Suwimol Jairtalawanich; Tinno Kwandee; Pichitchai Butnoi, "The effect of annealing temperature on properties of PZT ceramic films prepared via spin coating process," *Kasem Bundit Eng. J.*, vol. 13, no. 1, pp. 1–11, 2023.

[12]   P. K. Mahato, A. Seal, S. Garain, and S. Sen, "Effect of fabrication technique on the crystalline phase and electrical properties of PVDF films," *Mater. Sci.*, vol. 33, no. 1, pp. 157–162, 2015, doi: 10.1515/msp-2015-0020.

[13]   V. Reddy, S. K. Hulloli, and H. N. N. Murthy, "Development of PVDF Thin Films," *Int. J. Adv. Technol. Eng. Sci.*, vol. 4, no. 1, pp. 83–94, 2016.

[14]   X. Lu *et al.*, "Characterizations of P(VDF-HFP) -BaTiO3 nanocomposite films fabricated by a spin-coating process," *Ceram. Int.*, vol. 45, no. May, pp. 17758–17766, 2019.

[15] T. S. Roopaa, H. N. Narasimha Murthy, V. V. Praveen Kumar, and M. Krishna, "Development and characterization of PVDF thin films for pressure sensors," in *Materials Today: Proceedings*, Jan. 2018, vol. 5, no. 10, pp. 21082–21090, doi: 10.1016/J.MATPR.2018.06.503.

[16] I. Y. Abdullah, M. Yahaya, M. H. H. Jumali, and H. M. Shanshool, "Influence of the spinning rate on the β-phase formation in poly(vinylidene fluoride) (PVDF) films," *AIP Conf. Proc.*, vol. 1838, May 2017, doi: 10.1063/1.4982188.

[17] H. Kim, T. Fernando, M. Li, Y. Lin, and T. L. B. Tseng, "Fabrication and characterization of 3D printed BaTiO3/PVDF nanocomposites," *J. Compos. Mater.*, vol. 52, no. 2, pp. 197–206, Jan. 2018, doi: 10.1177/0021998317704709/ASSET/IMAGES/LARGE/10.1177_0021998317704709-FIG2.JPEG.

[18] T. Feng, D. Xie, Y. Zang, X. Wu, T. Ren, and W. Pan, "Temperature control of P(VDF-TrFE) copolymer thin films," *Integr. Ferroelectr.*, vol. 141, no. 1, pp. 187–194, 2013, doi: 10.1080/10584587.2012.694748.

[19] Y. Ting, Suprapto, N. Bunekar, K. Sivasankar, and Y. R. Aldori, "Using Annealing Treatment on Fabrication Ionic Liquid-Based PVDF Films," *Coatings 2020, Vol. 10, Page 44*, vol. 10, no. 1, p. 44, Jan. 2020, doi: 10.3390/COATINGS10010044.

[20] Y. Zheng, Q. Liu, X. Guan, Y. Liu, S. Nie, and Y. Wang, "Nitrogen Self-Doping Carbon Derived from Functionalized Poly(Vinylidene Fluoride) (PVDF) for Supercapacitor and Adsorption Application," *Micromachines*, vol. 13, no. 10, Oct. 2022, doi: 10.3390/MI13101747/S1.

[21] M. Satthiyaraju, T. Ramesh, and K. Jagatheswaran, "Annealing and ZnO Doping Effects on Hydrophilicity and Mechanical Strength of PVDF Nanocomposite Thin Films," *Lect. Notes Mech. Eng.*, pp. 463–471, 2019, doi: 10.1007/978-981-13-6374-0_52.

[22] R. Gregorio, and M. Cestari, "Effect of crystallization temperature on the crystalline phase content and morphology of poly(vinylidene fluoride)," *J. Polym. Sci. Part B Polym. Phys.*, vol. 32, no. 5, pp. 859–870, 1994, doi: 10.1002/POLB.1994.090320509.

[23] X. Cai, T. Lei, D. Sun, and L. Lin, "A critical analysis of the α, β and γ phases in poly(vinylidene fluoride) using FTIR," *RSC Adv.*, vol. 7, pp. 15382–15389, 2017, doi: 10.1039/c7ra01267e.

[24] P. Thakur, A. Kool, B. Bagchi, N. A. Hoque, S. Das, and P. Nandy, "In situ synthesis of Ni(OH)2 nanobelt modified electroactive poly(vinylidene fluoride) thin films: remarkable improvement in dielectric properties," *Phys. Chem. Chem. Phys.*, vol. 17, no. 19, pp. 13082–13091, May 2015, doi: 10.1039/C5CP01207D.

[25] S. Wu, J. Ning, F. Jiang, J. Shi, and F. Huang, "Ceramic Nanoparticle-Decorated Melt-Electrospun PVDF Nanofiber Membrane with Enhanced Performance as a Lithium-Ion Battery Separator," *ACS Omega*, vol. 4, no. 15, pp. 16309–16317, Oct. 2019, doi: 10.1021/ACSOMEGA.9B01541/ASSET/IMAGES/MEDIUM/AO9B01541_M005.GIF.

[26] S. Dowarah, D. Singh, and S. Kumar, "Formation and saturation of β-phase of PVDF in DMF solvent: a comprehensive study," Mar. 2024, doi: 10.21203/RS.3.RS-4022745/V1.

[27] Y. P. Su, L. N. Sim, H. G. L. Coster, and T. H. Chong, "Incorporation of barium titanate nanoparticles in piezoelectric PVDF membrane," *J. Memb. Sci.*, vol. 640, p. 119861, Dec. 2021, doi: 10.1016/J.MEMSCI.2021.119861.

[28] Y. Zhu *et al.*, "Effect of Annealing Temperatures and Time on Structural Evolution and Dielectric Properties of PVDF Films," *Polym. Polym. Compos.*, vol. 24, no. 2, pp. 167–172, 2016, doi: 10.1177/096739111602400213.

[29] I. Y. Abdullah, M. Yahaya, M. H. H. Jumali, and H. M. Shanshool, "Influence of the spinning rate on the β-phase formation in poly(vinylidene fluoride) (PVDF) films," *AIP Conf. Proc.*, vol. 1838, no. 1, May 2017, doi: 10.1063/1.4982188/749458.